BRAIN Initiative: Fast and Parallel Solver for Real-Time Monitoring of the Eddy Current in the Brain for TMS Applications

Abas Sabouni-*IEEE* Member, Philippe Pouliot-*IEEE* Member, Amir Shmuel-*IEEE* Member, and Frederic Lesage-*IEEE* Member

***Abstract*— This paper introduce a fast and efficient solver for simulating the induced (eddy) current distribution in the brain during transcranial magnetic stimulation procedure. This solver has been integrated with MRI and neuronavigation software to accurately model the electromagnetic field and show eddy current in the head almost in real-time. To examine the performance of the proposed technique, we used a 3D anatomically accurate MRI model of the 25 year old female subject.**

I. INTRODUCTION

Transcranial Magnetic Stimulation (TMS) is a technique which uses intense pulsed magnetic fields to induce currents in neuronal tissues which produce therapeutic effects in the brain [1]. If those currents are large enough, neurons can be locally depolarized. By localizing the magnetic field with prior anatomical MRI information, it is possible to modulate cortical function by exciting or inhibiting neuronal activity in a local area [2]. This technique is used today to treat neurological disorders such as depression [3]. It is also used to measure the connection between the primary motor cortex and a muscle, to evaluate damage from spinal cord injuries. Furthermore, these systems are also being investigated for treatment of a broad range of other neurological problems such as stroke, parkinsons disease, and schizophrenia [4]–[6]. Today, an electromagnetic coil is held against the forehead near an area of the brain that is thought to be involved in mood regulation. Then, short electromagnetic pulses are administered through the coil. The magnetic pulse easily passes through the skull, and causes small electrical currents that stimulate nerve cells in the targeted brain region [2]. The existing system has two disadvantages (i) During the TMS procedure, the user doesn't have any feedback of the pattern of activation induced in the brain and the amount of the induced current, and (ii) It is not possible to pinpoint a specific structure in the brain. The contribution of this paper is to propose fast and efficient TMS solver which allow the users to see the depth, location, and shape of the magnetic field in relation to the subject's brain on a computer monitor in real-time. Coupling the fast TMS with electroencephalography or other measurement techniques, it will be possible to observe the effects of currents in different locations and directions, to allow the circuitry of the brain to be understood. To the best of our knowledge, this is the first time that real-time TMS solver has been proposed.

Research supported by Wilkes University, CIHR, and NSERC Canada.

A. Sabouni is with Department of Electrical Engineering, Wilkes University, Wilkes-Barre, PA, 18766, USA (e-mail: abas.sabouni at wilkes.edu)

P. Pouliot is with the Biomedical Engineering Department, Ecole Polytechnique Montreal, Montreal, QC, H3C 3A7, Canada (e-mail: ph.pouliot at gmail.com)

A. Shmuel is with the Montreal Neurological Institute and Department of Biomedcical, McGill University, Montreal, QC, Canada (e-mail: amir.shmuel at mcgill.ca)

F. Lesage is with the Biomedical Engineering Department, Ecole Polytechnique Montreal, Montreal, QC, H3C 3A7, Canada (e-mail: frederic.lesage at polymtl.ca)

TABLE I
CONDUCTIVITY OF BRAIN TISSUES AT 3.3KHZ FREQUENCY

Tissue	GM	WM	CSF	Skull	Scalp
$\sigma(S/m)$	0.109	0.066	2.0	0.02	0.33

II. TMS CLINICAL TRIAL PROCEDURE

Fig. 1 shows a block diagram of the TMS system. To model induced current in a realistic brain, we used three dimensional (3D) Magnetic Resonance Imaging (MRI) of the brain (Fig. 2(a)). We used in-house MRI segmentation software to categorize different regions of the brain such as Scalp, Skull, Cerebro-Spinal Fluid (CSF), Gray Matter (GM), and White Matter (WM) (Fig. 2 (b)). This model was then inserted as input to the TMS simulator and conductivity values were assigned to each tissue type. Fig. 2 (c) and (d) show the cross-sectional view in sagittal and coronal planes of the segmented brain. The color bar in this figure indicate the different tissue type. Conductivity value of brain tissues have been investigated for many years and different researchers are reported different values for conductivity. In this paper, we used conductivity values reported in [7]. Table I show the conductivity values for each brain tissues at 3.3KHz frequency. The effect of tissue conductivity errors on the induced current has been investigated in [8]. The output of the neuronavigation system is also another input to the TMS simulator (FEM numerical solver) as shown in Fig. 1. A neuronavigation system (Brainsight ^{TM}) allowed the TMS coil to be navigated and positioned over a specified target location based upon an individual MRI image [9]. Therefore based on information from the neuronavigation system the position and orientation of the coil is determined and was then input to the TMS simulator to compute the expected flow of electric current in the brain. Results are then mapped on a MRI of the patient. The TMS simulator is explained in the following section.

978-1-4244-7929-0/14/$26.00 ©2014 IEEE

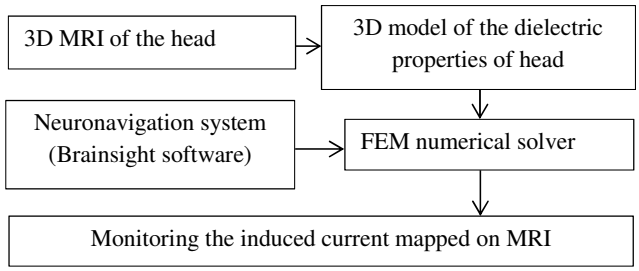

Fig. 1. Block diagram of the TMS system.

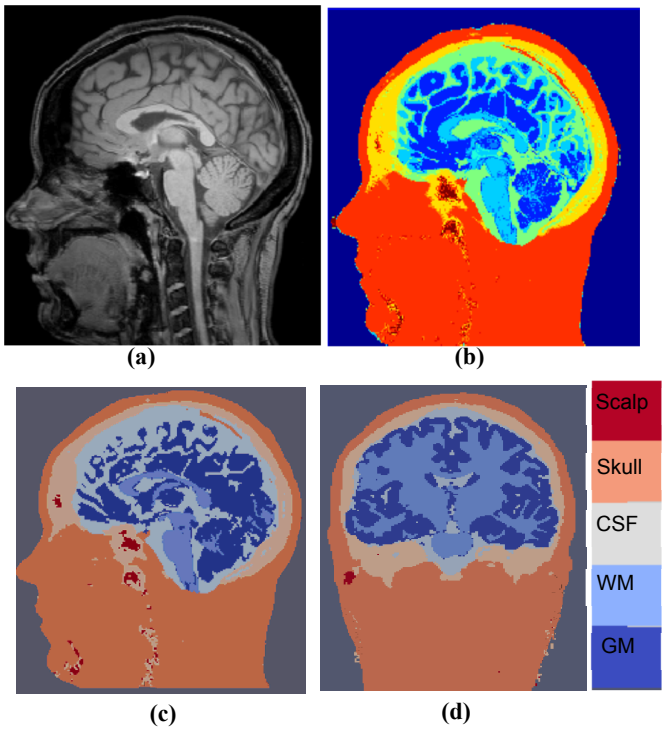

Fig. 2. (a) MRI date (b) Segmented MRI data, (c) Map of conductivity (sagittal plane), (d) Map of conductivity (coronal plane).

III. TMS SIMULATOR

The frequency range for TMS is from DC to 10kHz. In this range, the electromagnetic phenomenon satisfies Maxwell equations under quasi-static conditions. We used the so-called $T-\Omega$ formulation (current vector potential-magnetic scalar potential method) to model the electromagnetic propagation [10], [11]:

$$\nabla \times (\frac{1}{\sigma}\nabla \times \vec{T}) + j\omega\mu_0\vec{T} = -j\omega\mu_0\vec{H}_s + j\omega\mu_0\nabla\Omega \quad (1)$$

where j is the imaginary versor, ω is pulsation, $\vec{T}$ is the electric vector potential due to unknown currents in the head, $\nabla\Omega$ (magnetic scalar potential) represents field induced in the brain tissues, $\vec{H}_s$ is an external magnetic field (TMS coil), μ_0 is the permeability of free space, and σ is electric conductivity of the brain tissues. In (1) if $\vec{T}$ is known, then the eddy currents in the brain can be calculated as:

$$\nabla \times \vec{T} = \vec{J}_{ind} \quad (2)$$

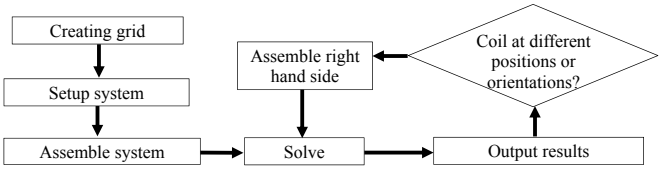

Fig. 3. Block diagram of the implementation of FEM code.

where $\vec{J}_{ind}$ is the induced current in the brain. Electromagnetic properties of the human head are considered to be low conducting ones [12]. Therefore the term $\nabla\Omega$ can be neglected in (1) [11]. The generated external field, $\vec{H}_s$ can be calculated everywhere outside the source using the Biot-Savart Law [13]. The partial differential equation (1) is solved by a vector Finite Element Method (FEM) capable of considering arbitrary complex geometries such as anatomical structures in the human brain [14]. In our proposed technique, an efficient and parallel FEM was implemented using C++ language and an object-oriented scientific library (Deal.II) [15]. In this technique instead of working with complex valued finite elements directly, we have split complex valued functions $\vec{T}$ into their real (T_r) and imaginary (T_j) parts (3) and use separate scalar finite element fields for discretizing each one of them. Therefore:

$$\vec{T} = T_r + jT_j \quad (3)$$

$$\nabla \times (\frac{1}{\sigma}\nabla \times T_r) - \omega\mu_0 T_j = \omega\mu_0 H_{sj} \quad (4)$$

$$\nabla \times (\frac{1}{\sigma}\nabla \times T_j) + \omega\mu_0 T_r = -\omega\mu_0 H_{sr} \quad (5)$$

where H_{sr} and H_{sj} are the real and imaginary part of the external magnetic field, respectively. Fig. 3 shows the block diagram of the implementation of FEM code for solving (4) and (5) individually. Deal.II library has a unique feature which is called dimension independent programming using C++ templates on locally adapted meshes which make the TMS solver more efficient programming. The proposed technique uses the same mesh in order to calculate the real and imaginary part of the electric vector potential. FEM has been used to solve the 3D TMS solver for a long time [11], [16]–[18], the progress in this field has been slow for a number of reasons - mainly insufficient computer power - which eventually solver it in an unreasonable amount of time. In recent years, tremendous research has been done on fast solver computing techniques and has opened up unique opportunities for future research. We used parallel computing with Message Passing Interface (MPI) in order to decrease the TMS solver run-time.

IV. RESULTS AND DISCUSSION

In order to show the capability of the proposed technique for calculating induced current, the MRI data from 25 year old healthy human subject has been used. The MRI data has been segmented in order to categorize different regions of the brain. The accuracy of induced eddy current depends on the quality of the segmentation. Fig. 4 shows map of conductivity

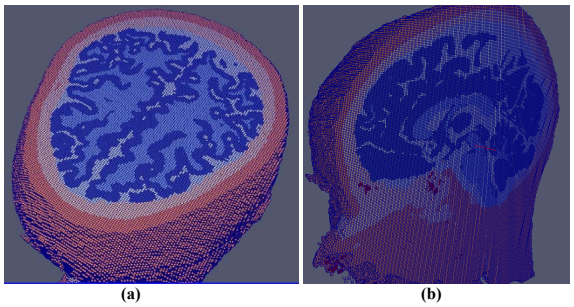

Fig. 4. (a) Map of conductivity (sagittal plane), (b) Map of conductivity (coronal plane) for 25 years old subject.

TABLE II
COMPARISON OF SIMULATION TIMES FOR DIFFERENT RESOLUTIONS

Resolution of Image	4mm	2mm
Degree of freedom	373,478	2,395,020
Number of coil Positions	61	61
Total CPU run-time	01:10:05	13:06:09
Number of machines	50	100
Memory usage	694,166,384kb	1,109,636,816kb

for this female subject. We have considered the circular coil to be used for stimulation. The coil is placed at the top of the head (Fig. 5), 2mm away from skin at five different locations as shown in Fig. 6. Figs. 7,8,9,10, and 11 show the induced current for A, B, C, D, and E locations of the coil in Fig. 6. The run-time of the TMS solver strongly depends on the resolution of the image. As the resolution of the induce current images increases the run-time also increases, because the number of unknown increases. Table II compares the simulation run-time for 61 positions of the coil for 2mm and 4mm image resolutions. The total CPU run-time for 2mm image resolution using 100 parallel machines took around 13 hours and for 4mm image resolution the CPU run-time took around 1 hour using 50 parallel machines.

Table III shows the run-time for each position (sample) of the coil for 2mm image resolution. As can be seen in this table, the first sample took around 10.5h, second sample around 30min, third sample 7.3min, forth sample 2.6min, and after that rest of the samples took only 41sec to be run. It is due to the fact that the mesh creating is usually the time consuming part of the FEM solver therefore the first sample take a lot of time to be solved. Then after that the run-time decreases rapidly and after 4th sample, by changing the coil position the eddy current image became ready in 40sec. Therefore in order to have real-time TMS solver, it is necessary to let solver to be run off-line, for at least few first samples, before TMS procedure started. Of course by increasing the number of the machine the simulation run-time decreases as shown in Table IV.

V. CONCLUSIONS

In this paper we introduced a fast and efficient TMS solver which read the MRI data to find out the segmentation of the brain and communicate with neuronavigation system. This

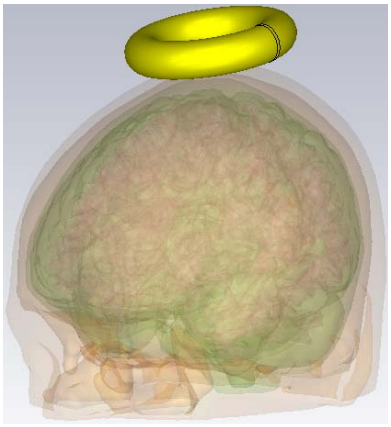

Fig. 5. Circular coil is placed at the top of the head.

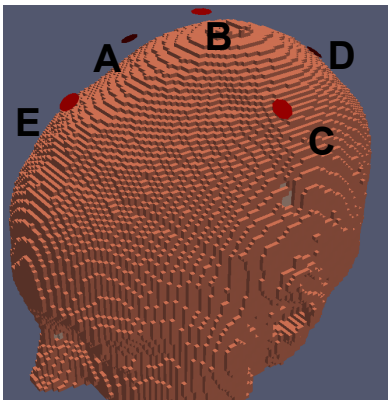

Fig. 6. Five different locations of the circular coil (A, B, C, D and E).

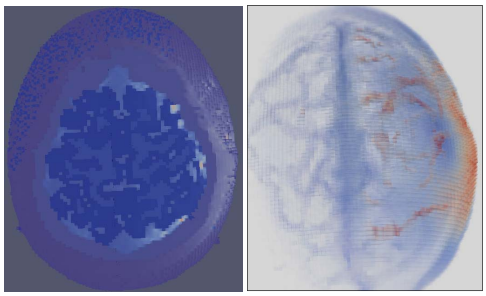

Fig. 7. Map of induced current for circular coil at A position Fig. 6. Right figure shows the map of induce current and left figure shows induce current mapped on the MRI (sagittal plane).

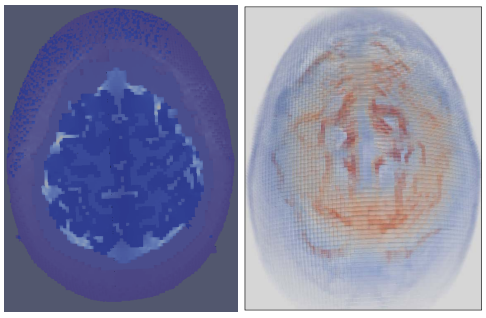

Fig. 8. Map of induced current for circular coil at B position Fig. 6. Right figure shows the map of induce current and left figure shows induce current mapped on the MRI (sagittal plane).

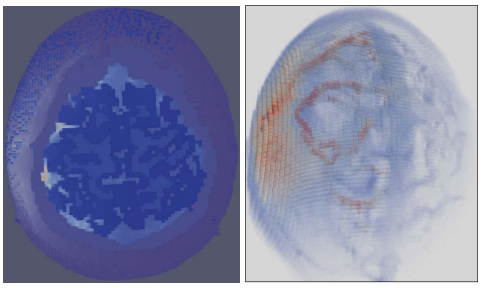

Fig. 9. Map of induced current for circular coil at C position in Fig. 6. Right figure shows the map of induce current and left figure shows induce current mapped on the MRI (sagittal plane).

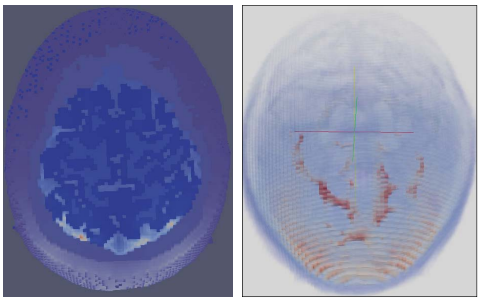

Fig. 10. Map of induced current for circular coil at D position in Fig. 6. Right figure shows the map of induce current and left figure shows induce current mapped on the MRI (sagittal plane).

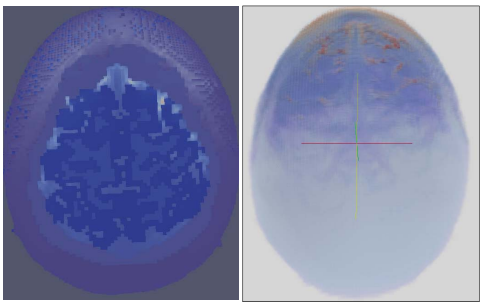

Fig. 11. Map of induced current for circular coil at E position in Fig. 6. Right figure shows the map of induce current and left figure shows induce current mapped on the MRI (sagittal plane).

TABLE III

SIMULATION RUN-TIME FOR CALCULATING EDDY CURRENT IN BRAIN WITH 2MM RESOLUTION

1 sample	≈10:32:00
2 sample	≈30 min
3 sample	≈7.3min
4 sample	≈2.6min
5-61 sample	≈41sec

TABLE IV

COMPARING THE RUN-TIME FOR TMS SOLVER FOR SAME RESOLUTION FOR DIFFERENT NUMBER OF MACHINES

Resolution of Image	2mm	2mm
Number of coil Positions	61	61
Number of machines	100	120
Memory usage	1,109,636,816kb	953,054,140kb
Total CPU run-time	13:06:09	11:21:11

solver allows users to see the depth, location, and shape of the magnetic field in relation to the subject's brain on a computer monitor in real-time. The fast TMS will enable the structure and function of the brain to be non-invasively probed by inducing electric current patterns on the surface of the brain and observing their effects on brain activity.

ACKNOWLEDGMENT

Authors would like to acknowledge the financial support of the Wilkes University, Canadian Institutes of Health Research, and the Natural Sciences and Engineering Research Council of Canada.

REFERENCES

[1] P. E. Holtzheimer and W. McDonald, Eds., *A Clinical Guide to Transcranial Magnetic Stimulation*. Oxford University Press, 2014.

[2] P. Rossini, L. Rosinni, and F. Ferreri, "Brain-behavior relations: Transcranial magnetic stimulation: A review," *Engineering in Medicine and Biology Magazine, IEEE*, vol. 29, no. 1, pp. 84 –96, jan.-feb. 2010.

[3] M. S. George, T. Schlaepfer, F. Padberg, and P. B. Fitzgerald, "Brain stimulation treatments for depression," *Biological Psychiatry*, vol. 15, pp. 167–168, 2014.

[4] E. Dammekensa, S. Vannesteb, J. Ostb, and D. D. Ridderb, "Neural correlates of high frequency repetitive transcranial magnetic stimulation improvement in post-stroke non-fluent aphasia: A case study," *Neurocase: The Neural Basis of Cognition*, vol. 20, pp. 1–9, 2014.

[5] R. Hanajima, Y. Teraoa, Y. Shirota, S. Ohminami, R. Tsutsumi, T. Shimizu, N. Tanaka, S. Okabe, S. Tsuji, and U. Y., "Triad-conditioning transcranial magnetic stimulation in parkinson's disease," *Brain Stimulation*, vol. 7, pp. 74–79, 2014.

[6] W. Strube, T. Wobrock, T. Bunse, U. Palm, F. Padberg, B. Malchow, P. Falkai, and A. Hasan, "Impairments in motor-cortical inhibitory networks across recent-onset and chronic schizophrenia: A cross-sectional tms study," *Behavioural Brain Research*, vol. 264, pp. 17–25, 2014.

[7] S. Gabriel, R. W. Lau, and C. Gabriel, "The dielectric properties of biological tissues: Iii. parametric models for the dielectric spectrum of tissues," *Physics in Medicine and Biology*, vol. 41, no. 11, p. 2271, 1996.

[8] A. Sabouni, "Effect of tissue conductivity errors on the induced current in transcranial magnetic stimulation (tms) of human brain," in *IEEE Antenna Propagation Conference (APS/URSI)*, 2014.

[9] *Brainsight TMS*, 1st ed., Rogue Research Inc, Montreal, Canada, 2007.

[10] Z. Ren, "T- omega; formulation for eddy-current problems in multiply connected regions," *IEEE Transactions on Magnetics*, vol. 38, no. 2, pp. 557 –560, mar 2002.

[11] J. Starzynski, B. Sawicki, S. Wincenciak, A. Krawczyk, and T. Zyss, "Simulation of magnetic stimulation of the brain," *Magnetics, IEEE Transactions on*, vol. 38, no. 2, pp. 1237 –1240, mar 2002.

[12] C. J. Stok, "The inverse problem in eeg and meg with application to the visual evoked responses," Ph.D. dissertation, University of Twente, Netherlands, 1986.

[13] J. R. Reitz, F. J. Milford, and R. W. Christy, *Foundations of Electromagnetic Theory*. Addison:Wesle, 1979.

[14] J. M. Jin, *The Finite Element Method in Electromagnetics*. New York: Wiley, 1993.

[15] W. Bangerth, R. Hartmann, and G. Kanschat, "Deal.ii - a general purpose object-oriented finite element library," *ACM Transactions on Mathematical Software*, vol. 33, no. 4, p. 24, 2007.

[16] T. Wagner, M. Zahn, A. J. Grodzinsky, and A. Pascual-Leone, "Three-dimensional head model simulation of transcranial magnetic stimulation," *Biomedical Engineering, IEEE Transactions on*, vol. 51, no. 9, pp. 1586–1598, Sept 2004.

[17] L. Golestanirad, M. Mattes, J. Mosig, and C. Pollo, "Effect of model accuracy on the result of computed current densities in the simulation of transcranial magnetic stimulation," *Magnetics, IEEE Transactions on*, vol. 46, no. 12, pp. 4046–4051, Dec 2010.

[18] J. van Welij, "Calculation of eddy currents in terms of h on hexahedra," *Magnetics, IEEE Transactions on*, vol. 21, no. 6, pp. 2239–2241, Nov 1985.